Vortex ring dynamics in trapped Bose-Einstein condensates

Matthew D. Reichl and Erich J. Mueller
Laboratory of Atomic and Solid State Physics, Cornell University, Ithaca, New York 14853, USA
(Received 26 September 2013; published 22 November 2013)

We use the time-dependent Gross-Pitaevskii equation to study the motion of a vortex ring produced by phase imprinting on an elongated cloud of cold atoms. Our approach models the experiments of Yefsah *et al.* [Nature (London) **499**, 426 (2013)] on ^{6}Li in the Bose-Einstein-condensate regime where the fermions are tightly bound into bosonic dimers. We find ring oscillation periods which are much larger than the period of the axial harmonic trap. Our results lend further strength to Bulgac *et al.*'s arguments (arXiv:1306.4266) that the "heavy solitons" seen in those experiments are actually vortex rings. We numerically calculate the periods of oscillation for the vortex rings as a function of interaction strength, trap aspect ratio, and minimum vortex ring radius. In the presence of axial anisotropies the rings undergo complicated internal dynamics where they break into sets of vortex lines, then later combine into rings. These structures oscillate with a similar frequency to simple axially symmetric rings.

DOI: 10.1103/PhysRevA.88.053626 PACS number(s): 67.85.Lm, 67.85.De, 03.75.Lm

I. INTRODUCTION

Yefsah *et al.* [1] recently observed anomalously slow oscillations of a nominal soliton in a harmonically trapped fermionic superfluid. By illuminating half the cloud with light, they generated a phase profile with a large jump. This phase jump evolved into a localized density depletion that oscillated with a period many times larger than the period associated with the harmonic trap. This slow motion is remarkable, as it exceeds previous theoretical calculations of the oscillation frequency of a soliton [2,3] by an order of magnitude. Recently, Bulgac *et al.* [4] hypothesized that the experimental protocol produces a vortex ring instead of a soliton. Through integrating time-dependent equations based upon a superfluid density-functional theory, Bulgac *et al.* showed that near unitarity the experimental observations are consistent with this vortex ring hypothesis. Here we extend this analysis to the Bose-Einstein-condensate (BEC) regime, where the fermions are tightly bound into dimers.

To study this problem, we numerically evolve the time-dependent Gross-Pitaevskii (GP) equation to simulate the dynamics of vortex rings. We model the phase-imprinting process and measure the period of oscillations of the vortex ring as a function of interaction strength, trap aspect ratio, and initial ring radius. We find that the period of oscillation for the vortex ring is quantitatively consistent with the experimental observations in the BEC regime.

In our simulations, the phase imprinting produces a soliton [5] that decays into a vortex ring through a "snake instability." This instability has been explored in the past [5–9], as has the structure and motion of individual vortex rings [10–22]. Here we explore the full process in an elongated trap. An excellent review of the theory of solitons and vortices in BECs can be found in Ref. [23].

Experimentally, vortex rings have been observed in the decay of dark solitons [24], in complex vortex-ring–soliton oscillations [25,26], and in binary condensates [27].

II. PHYSICS OF VORTEX RINGS

The flow in a Bose-Einstein condensate is irrotational ($\nabla \times \mathbf{v} = 0$, where $\mathbf{v} = \frac{\hbar}{m}\nabla\phi$ is the local velocity and ϕ is the phase of the order parameter) except at line singularities. The superfluid phase winds by $2\pi n$, for integer n, when one moves around one of these vortex lines. Here we study configurations where these vortex lines form loops. In particular, consider a cigar-shaped cloud, elongated along the $\hat{z}$ axis, with a vortex ring in a perpendicular plane, concentric with the cloud. In Sec. III we numerically solve the time-dependent GP equation to analyze such a ring, but its basic properties can be understood from a semiclassical argument given by Jackson *et al.* [18] for a vortex ring in a spherically symmetric condensate. They find that each element of the vortex ring moves with a velocity $\mathbf{v}$:

$$\mathbf{v} = v_{\rm in}(R)\hat{\mathbf{z}} + \omega_p \hat{\kappa} \times \mathbf{r}, \tag{1}$$

where $\hat{\kappa}$ defines the direction of the circulation at the element.

The first term in Eq. (1) describes the induced velocity $v_{\rm in}(R)$ resulting from the sum of the velocity contributions from each element on the ring. For a ring in a uniform condensate, this induced velocity is a function of the ring radius R and is given by $v_{\rm in}(R) = \frac{\hbar}{2mR}[\ln(8R/\xi) - 0.615]$ [14], where ξ is the coherence length. Thus the ring has an inherent tendency to propagate along the z axis.

A cartoon of this physics comes from the two-dimensional analog of a vortex ring: a vortex dipole consisting of two point vortices: one with circulation $+\kappa$ and the other with $-\kappa$. If these are separated by a distance $2R$, they move with a velocity $v = \frac{\kappa}{4\pi R}$ [28].

The second term in Eq. (1) describes the Magnus force on the ring caused by the harmonic trap. In the case of a straight vortex line, this force leads to precession with frequency ω_p. Note that w_p is not equal to any trap frequency; for instance, in the Thomas-Fermi limit, a single vortex in a two-dimensional condensate will precess with a frequency given by [29]

$$\omega_p = \frac{3\hbar\omega^2}{4\mu}\ln\left(\frac{R_\perp}{\xi}\right), \tag{2}$$

where ω is the trap frequency, $\mu = \hbar^2/2m\xi^2$ and $R_\perp^2 = 2\mu/m\omega^2$.

A small ring ($R \ll R_\perp$) beginning at $z = 0$ will have a large velocity component in the positive z direction. As it

moves in the z direction, the Magnus term, $\hat{\kappa} \times \mathbf{r}$, causes the ring to grow. Once the ring radius is sufficiently large, the Magnus force pushes the ring in the negative z direction. In this manner the ring moves periodically. The two-dimensional analog of this motion was observed in experiments by Neely *et al.* [30].

While this model is too simple to produce a quantitative prediction for the period of these vortex ring oscillations, it captures the qualitative behavior of the vortex ring seen in the numerical simulations discussed in Sec. III C. Moreover, it predicts that the period should increase roughly as $T_{\text{ring}} \sim \frac{1}{\xi^2 \ln(1/\xi)} \sim gn/\ln gn \sim g^{2/5}/\ln g$, where g is the interaction strength and n is the density. This scaling is seen in our simulations (see Fig. 3). We note that the period of dark-soliton oscillations, $T_{\text{sol}} = \sqrt{2}T_z$ [31–33], where T_z is the trap period in the z direction, is independent of g. For sufficiently large g we expect slower oscillations for the vortex ring than the dark soliton.

We also note that the vortex ring dynamics are highly nonlinear and that the ring's oscillation period is strongly dependent on the minimum ring radius. As in Bulgac *et al.*'s work [4], we find that smaller radii lead to shorter periods (see Fig. 5). We also find that the oscillations are nonsinusoidal, with a slight asymmetry between the motion to the left and to the right.

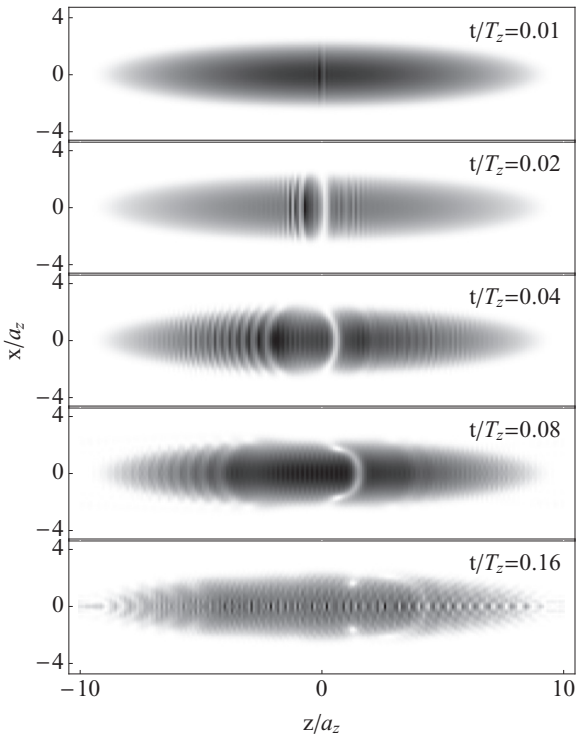

FIG. 1. Condensate dynamics following phase imprinting with $g = 4000$, $\lambda = 4$. Each graph shows the density $|\psi(x, y = 0, z)|^2$, where darker colors represent higher density. The dark soliton is unstable and forms a vortex ring (seen as two zero-density cores) at time $t/T_z \approx 0.16$

III. NUMERICAL RESULTS

A. Simulation details

In this section we present results from numerical simulations of the time-dependent GP equation:

$$i\hbar\partial_t\psi = -\frac{\hbar^2}{2m}\nabla^2\psi + V_t(r,z)\psi + \frac{4\pi\hbar^2 aN}{m}|\psi|^2\psi + V_i(t,r,z)\psi, \tag{3}$$

where N is the total number of particles, a is the scattering length, and ψ is normalized such that

$$\int |\psi(\vec{r})|^2 d^3r = 1. \tag{4}$$

$V_t(r,z) = \frac{m}{2}(\omega_r^2 r^2 + \omega_z^2 z^2)$ is a harmonic trapping potential, and $V_i(t,r,z)$ is a time-dependent phase-imprinting potential, which we will describe below.

After rescaling the variables $t \to \omega_z t$, $\vec{r} \to \frac{1}{a_z}\vec{r}$ where $a_z = \sqrt{\frac{\hbar}{m\omega_z}}$, and rescaling $\psi \to a_z^{3/2}\psi$, we can rewrite the GP equation in the dimensionless form:

$$i\partial_t\psi = -\tfrac{1}{2}\nabla^2\psi + g|\psi|^2\psi + \tfrac{1}{2}(\lambda^2 r^2 + z^2)\psi + V_i(t,r,z)\psi, \tag{5}$$

where $\lambda = \frac{\omega_r}{\omega_z}$ is the trap aspect ratio and $g = \frac{4\pi aN}{a_z}$ parametrizes the interaction strength. As discussed in Sec. III C, an experimentally relevant set of parameters is $\lambda = 6$ and $g = 3 \times 10^4$.

In Secs. III B and III C we assume axial symmetry, while in Sec. III D we carry out full three-dimensional (3D) simulations, including slight trap asymmetries. We numerically solve Eq. (5) using a split-step method. We use a square grid, choosing our grid spacing sufficiently small that the dynamics are independent of the grid. We find for our parameter range that it suffices to take $\delta r = \delta z = 0.1$. Smaller grids are necessary for larger interactions. Similarly, we find a time step $\delta t = 10^{-3}$ suffices for preventing large phase jumps between time steps, ensuring numerical stability. We set $V_i(t,r,z) = \frac{\pi}{\delta t}\Theta(t)\Theta(\delta t - t)f(z)$ so that a sharp ϕ phase jump is imprinted about the line $z = 0$ after the first time step. Each simulation begins after first relaxing the system into the ground state of the trapping potential using imaginary-time propagation.

The resulting dynamics after phase imprinting can depend sensitively on the precise shape of $f(z)$. However, away from the quasi-one-dimensional regime ($\lambda \ll ng$), we find from our simulations that $f(z)$ generically creates a soliton that quickly decays into one (as in Fig. 1) or more vortex rings via a snake instability. For simplicity and in keeping with the experimental observations in Ref. [1] where there is only one discernible density depletion, we choose $f(z) = \frac{1}{2}[1 + \tanh(z/\delta z)]$, where δz is our numerical grid spacing. This protocol consistently results in only one long-lasting vortex ring.

It is difficult to control the minimum radius R_{min} of the vortex ring using this phase-printing technique. Therefore, to study the behavior of the vortex ring as function of R_{min}, we do not use phase imprinting but instead relax the gas to a state with the following ansatz for its phase:

$$\frac{\psi(r,z)}{|\psi(r,z)|} = \frac{(r - R_{\text{min}}) + iz}{\sqrt{(r - R_{\text{min}})^2 + z^2}}. \tag{6}$$

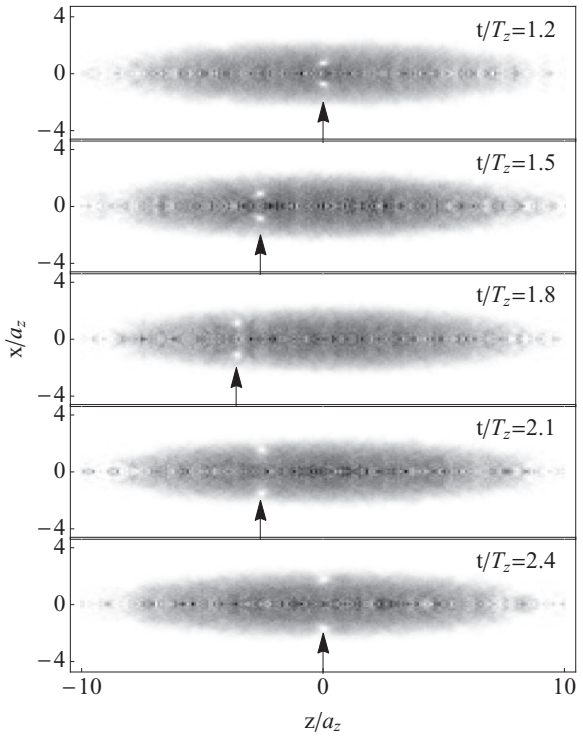

FIG. 2. Half of a vortex ring oscillation with $g = 4000$, $\lambda = 4$. Each graph shows the density $|\psi(x, y = 0, z)|^2$, where darker colors represent higher density. An arrow is shown pointing to the vortex ring.

This ansatz closely approximates the phase of the vortex rings created after phase imprinting and allows us to easily investigate the ring behavior as a function of $R_{\min}$.

B. Example of snake instability and vortex ring dynamics

Figure 1 shows an example of the dynamics of the condensate following phase imprinting. A soliton, seen as a density dip extending axially through the condensate, travels in the positive z direction and almost immediately begins bowing outward near the center of the gas (see $t/T_z = 0.04$ in Fig. 1). By time $t/T_z = 0.16$ the soliton has decayed via this snake instability, leaving a vortex ring which is seen as two zero-density cores in the $y = 0$ slice shown in Fig. 1.

Figure 2 shows an example of the vortex ring oscillations that follow the decay of a soliton. At $t/T_z \approx 1.2$ the vortex ring is positioned at $z = 0$ and is traveling in the negative z direction. The ring continues to travel in this direction until $t/T_z \approx 1.8$. After this time the ring radius expands to the edge of condensate while the ring begins traveling back in the positive z direction. The ring completes half of an oscillation and returns to $z = 0$ at $t/T_z \approx 2.4$. In the following section we calculate the frequency of vortex ring oscillations as a function of g, λ, and $R_{\min}$.

C. Period of vortex ring oscillations

Figure 3 shows a plot of the vortex ring oscillation period as a function of interaction strength g with a trap aspect ratio of $\lambda = 4$. Each point is computed by first preparing the vortex ring with the phase-imprinting method discussed in Sec. III A

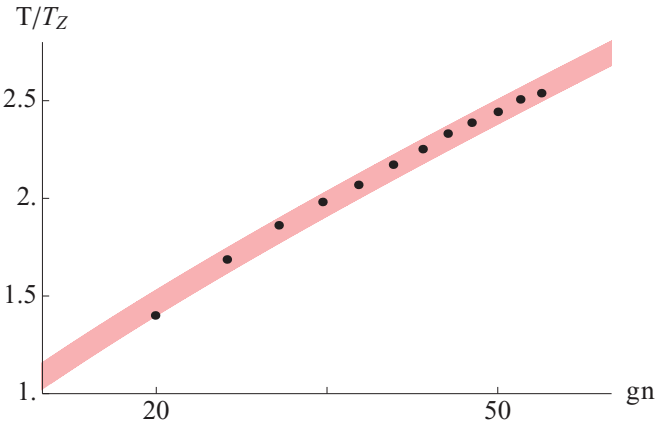

FIG. 3. (Color online) Vortex ring oscillation period T (normalized by the trap period T_z) vs interaction strength times the density gn with a trap aspect ratio of $\lambda = 4$ after phase imprinting. As predicted in Sec. II, $T \sim gn/\ln gn$; the thick red curve shows a fit of the data to this scaling.

and then calculating the number of time steps for a vortex core starting at $z = 0$ to complete an oscillation and return to $z = 0$. As predicted above, the oscillation period increases as $gn/\ln gn$ for large gn. Moreover, for $g \gtrsim 500$, the vortex ring oscillates at a period larger than the period for a dark soliton in a BEC $T = \sqrt{2}T_z$ [31–33].

In Fig. 4 we plot the oscillation period of the ring as a function of trap aspect ratio λ at constant interaction strength $g = 4000$. The period decreases at larger aspect ratios, which is consistent with observations in Ref. [1]. The explanation for this trend is that our phase-imprinting method yields vortex rings with smaller minimum radii at larger λ. As discussed in Sec. II, the rings with smaller $R_{\min}$ have smaller periods.

To explore the radius dependence of the ring dynamics, we find the ring oscillation period as a function of $R_{\min}$ [see Eq. (6)] with $g = 4000$ and $\lambda = 4$ using the relaxation procedure discussed in the last paragraph of Sec. III A. The results are shown in Fig. 5, which clearly demonstrates that

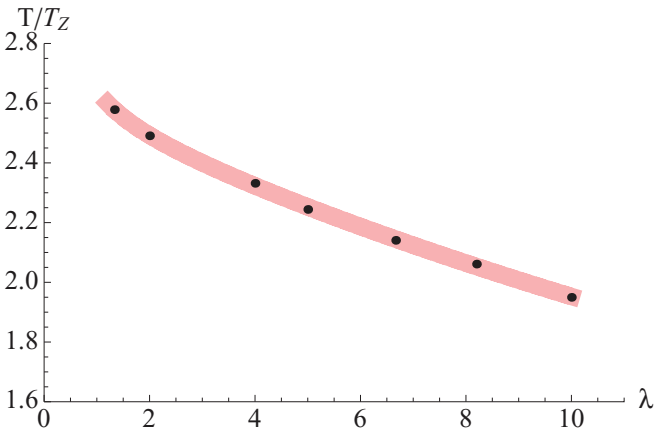

FIG. 4. (Color online) Vortex ring oscillation period T (normalized by the trap period T_z) vs trap aspect ratio $\lambda = \frac{\omega_r}{\omega_z}$ after phase imprinting with $g = 4000$. The thick red curve is an interpolation to guide the eye.

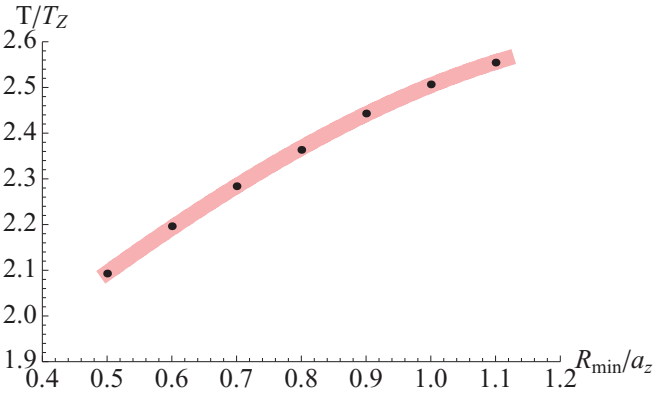

FIG. 5. (Color online) Vortex ring oscillation period T (normalized by the trap period T_z) vs the minimum vortex ring radius $R_{\min}$ with $g = 4000$ and $\lambda = 4$. The thick red curve is an interpolation to guide the eye.

rings with smaller $R_{\min}$ have smaller periods; this is consistent with a similar finding reported in Ref. [4].

Finally, we compare our simulations to the experiment in Ref. [1]. Typical experimental parameters in the BEC regime are $T_r \approx 14$ ms, $T_z \approx 87$ ms, total number of bosonic Feshbach molecules $N \approx 1.1 \times 10^5$, Thomas-Fermi radius $R_{TF} = (R_{TF_x} R_{TF_y} R_{TF_z})^{1/3} = 135\ \mu$m, and $\frac{1}{k_F a_F} \approx 2.6$, where $k_F \approx 0.86\ \mu\text{m}^{-1}$ is the Fermi wave vector and $a_F \approx 0.448\ \mu$m is the fermionic scattering length at $B = 700G$. Noting that $a = 0.6 a_F$ [34], these parameters give $\lambda = 6.2$ and $g = 3.08 \times 10^4$ in our dimensionless units.

We find that with these parameters the soliton created after phase imprinting quickly decays into a vortex ring. The period depends sensitively on the minimum ring radius (as in Fig. 5), which in turn depends on the phase-imprinting protocol. We can reproduce (within the reported error bars) the experimentally measured period of $T = 4.4 \pm 0.5 T_z$ by relaxing to a vortex ring state using the ansatz in Eq. (6) with $R_{\min} = 1.2 a_z$. It is plausible that the particular phase imprinting procedure used in the experiment yields a vortex ring with a similar minimum ring radius.

D. Ring dynamics with axial asymmetry

To give a more complete picture, we relaxed our assumption of axial asymmetry and performed fully three-dimensional simulations with a trap potential given by $V_t(x,y,z) = \frac{1}{2}[\lambda^2(0.99x^2 + y^2) + z^2]$. We again find the vortex structure moves periodically in the z direction (with roughly the same period), but we find additional internal dynamics, some of which is related to previous studies [35,36].

This evolution is illustrated by Fig. 6(a), which shows the locations of nonzero vorticity at different times projected into the x-y plane (here $\lambda = 4$, $g = 4000$). Figure 6(b) shows the density of the condensate integrated over the x and y directions. The system at time $t = 0$ contains a vortex ring of radius $R = 1.0 a_z$ located at $z = 0$. After one half of an oscillation (at $t/T_z \approx 1.4$) the vortex ring breaks apart into two lines of opposite vorticity extending along the x axis, which continue to move together along the z axis. After reaching the edge of the condensate, the vortex lines recombine into a ring which then moves in the opposite direction along the z axis. Similar behavior is seen over the range of parameters explored in Sec. III C. From the axial density profiles in Fig. 6(b), however,

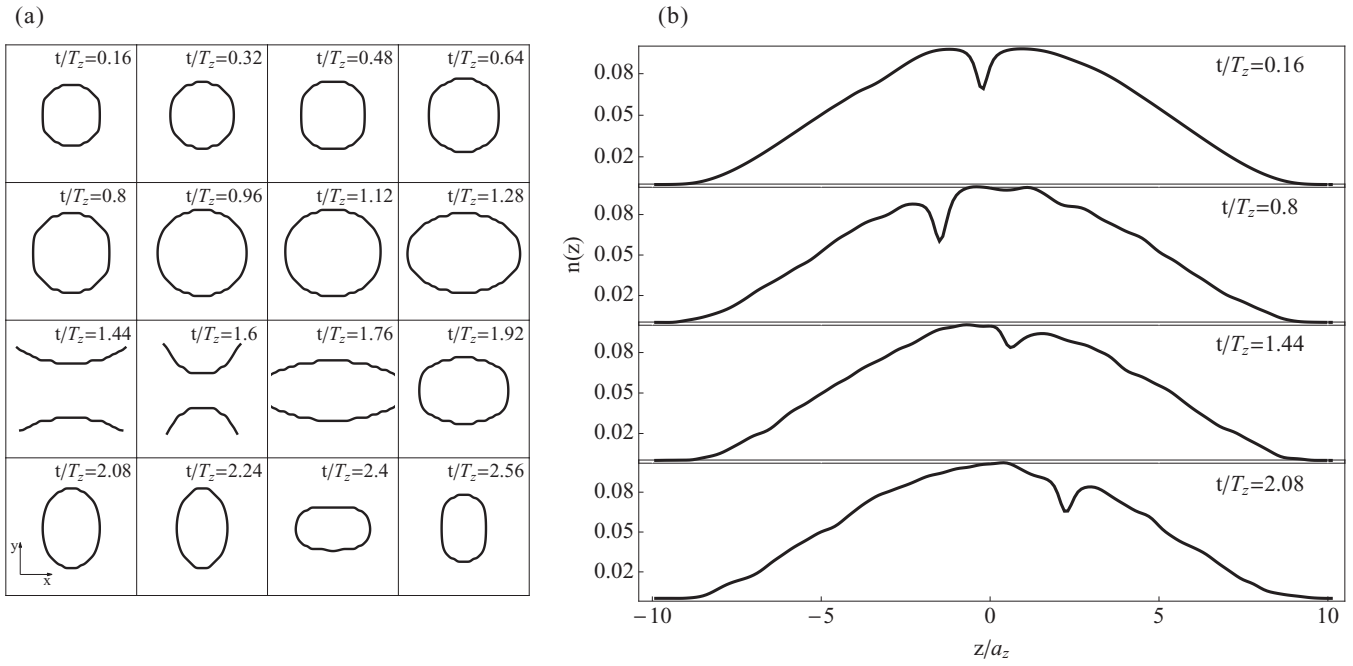

FIG. 6. Vortex ring dynamics in the presence of a small perturbation to axial symmetry ($V_t(x,y,z) = \frac{1}{2}[\lambda^2(0.99x^2 + y^2) + z^2]$). Here $\lambda = 4$, $g = 4000$, and the system is initialized with a vortex ring of radius $R = 1.0 a_z$ located at $z = 0$. (a) The locations of nonzero vorticity at different times projected into the x-y plane. (b) The density of the condensate at different times integrated over the x and y directions, $n(z) = \int dx dy \rho(x,y,z)$.

none of this internal dynamics is apparent. In fact Fig. 6(b) looks like an oscillating gray soliton.

IV. CONCLUSION

Using numerical simulations, we have found that dark solitons created through phase imprinting in three-dimensional BECs are unstable to become vortex rings and that these vortex rings oscillate with much larger periods than solitons. We numerically computed the period of these vortex ring oscillations as a function of interaction strength, trap aspect ratio, and minimum vortex ring radius. We found that our results are qualitatively consistent with Jackson *et al.*'s [18] semiclassical model of vortex rings for axially symmetric potential traps. Slight perturbations to axial symmetry produce negligible changes to the oscillation period of the ring but cause the ring to break apart and recombine during oscillations. Finally, we simulate the BEC regime of a recent experiment claiming to have observed oscillations of "heavy" dark solitons in cold Fermi gases [1]. The oscillation periods of vortex rings in our simulations are quantitatively consistent with the periods of the supposed solitons, and we therefore conclude that these solitons are likely to be vortex rings or more complicated objects, as shown in Fig. 6.

A key distinction between vortex rings and solitons, besides their dynamics, is their density profile: a vortex ring appears as two density dips in a two-dimensional profile, while a soliton appears as a solid line of density depletion extending across the condensate. In fermionic superfluids away from the BEC regime, the density depletion associated with vortices and solitons is small, as the cores are filled by normal fluid. For superfluids initially away from the BEC regime, Yefsah *et al.* [1] were forced to ramp the magnetic field to the deep BEC regime in order to clearly observe *any* density depletion in their gas after releasing it from the trap. We recommend further experiments in the BEC regime where such ramps are unnecessary. We note that previous experiments with BECs have successfully distinguished vortex rings from dark solitons using expansion imaging [24] and *in situ* imaging [26]. We also note that several of the images in Ref. [1] are suggestive of vortex rings or tangles. This is particularly true of the images in the supplementary information section.

A less direct distinguishing feature of a vortex ring's dynamics is the asymmetry of its motion. For example, if the ring is smaller when moving left to right, it will move faster during that interval than on the return. In Fourier analysis of the existing experimental data, this asymmetry would show up as odd harmonics. We calculated the first odd harmonic for the experimental parameters and, unfortunately, found it too small to readily measure. Devising techniques to generate vortex rings with a smaller minimum radius would improve this situation.

Finally, we should mention one shortcoming of our modeling. We find that for our axially symmetric simulations the period of the vortex ring is sensitive to the imprinting protocol, while the experiment finds very reproducible periods. Perhaps the more complicated structures in Sec. III D yield more reproducibility. The computational cost of the full 3D simulations have prevented us from studying this in detail.

ACKNOWLEDGMENTS

We thank Martin Zwierlein and Waseem Bakr for discussions and correspondence. We thank Francesco Piazza for making comments leading to our study of the axially anisotropic case. We thank Alexander Fetter for small corrections regarding the two-dimensional analog system. This material is based upon work supported by the National Science Foundation Graduate Research Fellowship under Grant No. DGE-1144153 as well as work supported by the National Science Foundation under Grant No. PHY-1068165.

[1] T. Yefsah, A. T. Sommer, M. J. Ku, L. W. Cheuk, W. Ji, W. S. Bakr, and M. W. Zwierlein, Nature (London) **499**, 426 (2013).
[2] R. Liao and J. Brand, Phys. Rev. A **83**, 041604 (2011).
[3] R. G. Scott, F. Dalfovo, L. P. Pitaevskii, and S. Stringari, Phys. Rev. Lett. **106**, 185301 (2011).
[4] A. Bulgac, M. M. Forbes, K. J. Roche, and G. Wlazłowski, arXiv:1306.4266, Phys. Rev. Lett. (to be published).
[5] D. Frantzeskakis, J. Phys. A **43**, 213001 (2010).
[6] E. A. Kuznetsov and J. J. Rasmussen, Phys. Rev. E **51**, 4479 (1995).
[7] A. Muryshev, H. B. van Linden van den Heuvell, and G. V. Shlyapnikov, Phys. Rev. A **60**, R2665 (1999).
[8] D. L. Feder, M. S. Pindzola, L. A. Collins, B. I. Schneider, and C. W. Clark, Phys. Rev. A **62**, 053606 (2000).
[9] A. Cetoli, J. Brand, R. G. Scott, F. Dalfovo, and L. P. Pitaevskii, Phys. Rev. A **88**, 043639 (2013).
[10] K. Shariff and A. Leonard, Annu. Rev. Fluid Mech. **24**, 235 (1992).
[11] G. K. Batchelor, *An Introduction to Fluid Dynamics* (Cambridge University Press, Cambridge, 2000).
[12] G. W. Rayfield and F. Reif, Phys. Rev. **136**, A1194 (1964).
[13] D. Amit and E. Gross, Phys. Rev. **145**, 130 (1966).
[14] P. Roberts and J. Grant, J. Phys. A **4**, 55 (1971).
[15] C. Jones and P. Roberts, J. Phys. A **15**, 2599 (1982).
[16] R. J. Donnelly, *Quantized Vortices in Helium II* (Cambridge University Press, Cambridge, 1991), Vol. 2.
[17] J. Koplik and H. Levine, Phys. Rev. Lett. **76**, 4745 (1996).
[18] B. Jackson, J. F. McCann, and C. S. Adams, Phys. Rev. A **61**, 013604 (1999).
[19] M. Guilleumas, D. M. Jezek, R. Mayol, M. Pi, and M. Barranco, Phys. Rev. A **65**, 053609 (2002).
[20] C. Hsueh, S.-C. Gou, T. Horng, and Y.-M. Kao, J. Phys. B **40**, 4561 (2007).
[21] M. Abad, M. Guilleumas, R. Mayol, and M. Pi, Laser Phys. **18**, 648 (2008).
[22] R. M. Caplan, CGU Thesis & Dissertations, Claremont Colleges, CA, 2012.
[23] R. Carretero-González, D. Frantzeskakis, and P. Kevrekidis, Nonlinearity **21**, R139 (2008).

[24] B. P. Anderson, P. C. Haljan, C. A. Regal, D. L. Feder, L. A. Collins, C. W. Clark, and E. A. Cornell, Phys. Rev. Lett. **86**, 2926 (2001).
[25] N. S. Ginsberg, J. Brand, and L. V. Hau, Phys. Rev. Lett. **94**, 040403 (2005).
[26] I. Shomroni, E. Lahoud, S. Levy, and J. Steinhauer, Nat. Phys. **5**, 193 (2009).
[27] K. M. Mertes, J. W. Merrill, R. Carretero-González, D. J. Frantzeskakis, P. G. Kevrekidis, and D. S. Hall, Phys. Rev. Lett. **99**, 190402 (2007).
[28] D. Pelinovsky and P. Kevrekidis, Nonlinearity **24**, 1271 (2011).
[29] A. L. Fetter and A. A. Svidzinsky, J. Phys. Condens. Matter **13**, R135 (2001).
[30] T. Neely, E. Samson, A. Bradley, M. Davis, and B. Anderson, Phys. Rev. Lett. **104**, 160401 (2010).
[31] T. Busch and J. R. Anglin, Phys. Rev. Lett. **84**, 2298 (2000).
[32] V. V. Konotop and L. Pitaevskii, Phys. Rev. Lett. **93**, 240403 (2004).
[33] C. Becker, S. Stellmer, P. Soltan-Panahi, S. Dörscher, M. Baumert, E.-M. Richter, J. Kronjäger, K. Bongs, and K. Sengstock, Nat. Phys. **4**, 496 (2008).
[34] D. S. Petrov, C. Salomon, and G. V. Shlyapnikov, Phys. Rev. Lett. **93**, 090404 (2004).
[35] T.-L. Horng, S.-C. Gou, and T.-C. Lin, Phys. Rev. A **74**, 041603 (2006).
[36] F. Piazza, L. Collins, and A. Smerzi, New J. Phys. **13**, 043008 (2011).